Available online at www.sciencedirect.com
SCIENCE DIRECT®
Analytical Biochemistry 336 (2005) 64–74
ANALYTICAL BIOCHEMISTRY
www.elsevier.com/locate/yabio

Evaluation of two lanthanide complexes for qualitative and quantitative analysis of target proteins via partial least squares analysis

Hector Goicoechea[a,1], Bidhan C. Roy[b], Marina Santos[a], Andres D. Campiglia[a,*], Sanku Mallik[b]

[a] Department of Chemistry, University of Central Florida, P.O. Box 25000, Orlando, FL 32816-23366, USA
[b] Department of Chemistry and Molecular Biology, North Dakota State University, Fargo, ND 58105, USA

Received 7 July 2004
Available online 5 November 2004

Abstract

Two lanthanide complexes, namely 5-aminosalicylic acid ethylenediaminetetraacetate europium(III) (5As-EDTA-Eu^{3+}) and 4-aminosalicylic acid ethylenediaminetetraacetate terbium(III), were evaluated for the analysis of carbonic anhydrase, human serum albumin (HSA), and γ-globulin. Quantitative analysis is based on their luminescence enhancement upon protein binding and qualitative analysis on their lifetime capability to recognize the binding protein. Analytical figures of merit are presented for the three proteins. The limits of detection with 5As-EDTA-Eu^{3+} are at the parts per billion level. Partial least square regression analysis is used to determine HSA and γ-globulin in binary mixtures without previous separation at the concentration ranges typically found in clinical tests of human blood serum.

Keywords: Luminescence; Lanthanide ions; Carbonic anhydrase; γ-Globulin; Human serum albumin; Partial least squares regression; Proteins

The development of methodology for protein recognition and quantification in complex biological matrices has long been an analytical challenge. The limitations of popular clinical and laboratory tests have been extensively discussed in the literature [1]. The Lowry [2] and the Bradford [3,4] methods, which determine total protein content, lack selectivity for specific protein determination. Spectrophotometric [5,6], chemiluminescence [7,8], fluorimetric [9,10] and resonance light scattering [11,12] methods have shown distinct improvement over classical assays. Their main advantages include accuracy of analysis and better limits of detection. Their selectivity, however, still falls short for the problem at hand. Other trends, which combine mass spectrometry to liquid chromatography [13,14] or electrophoresis [15,16], provide excellent selectivity and sensitivity but require elaborate sample separation prior to protein determination.

Selectivity improvements for direct protein determination have been recently reported with synchronous fluorescence [1] and near-infrared [17,18] spectroscopy. The fluorescence assay [1] relies on chemical interactions among targeted proteins and functionalized nanoparticles. The spectral response of a fluorescence tag chemically attached to nanoparticles is monitored via synchronous excitation to extract both qualitative and quantitative information. The near-infrared approach [17,18] takes advantage of vibrationally resolved spectra with fingerprint information for protein identification.

* Corresponding author. Fax: +1 407 823 2252.
E-mail address: acampigl@mail.ucf.edu (A.D. Campiglia).
[1] Present address: Catedra de Quimica Analitica I, Facultad de Bioquímica y Ciencias Biológicas, Universidad Nacional del Litoral, Ciudad Universitaria, CC 242-S30001 Santa Fe, Argentina.

0003-2697/$ - see front matter © 2004 Elsevier Inc. All rights reserved.
doi:10.1016/j.ab.2004.09.020

Because near-infrared absorption bands are inherently weak, spectral assignment is made possible with the aid of chemometric methods that minimize spectral interference from instrumental noise and sample concomitants.

Our approach focuses on chemical receptors with the potential to recognize specific proteins in complex samples. We incorporate lanthanide ions into polymerized liposomes that offer a lipophilic platform for protein interaction with the lanthanide ion [19,20]. The specificity of our approach relies on the capability of the polymerized liposome to recognize a specific protein in the complex sample. The expectation from the lanthanide ion is to report qualitative and quantitative information on the interacting protein(s), even if the target protein(s) is at much lower concentration than sample concomitants. In this article, we present a thorough investigation of two lanthanide complexes and their analytical potential as luminescence reporters for liposome–protein interaction. We first describe their synthetic preparation and then evaluate their quantitative and qualitative performance for three targeted proteins, namely carbonic anhydrase (CA),[2] human serum albumin (HSA), and γ-globulin. With the aid of partial least squares (PLS) regression, we demonstrate the feasibility to determine HSA and γ-globulin in binary mixtures at the concentration levels typically found in human blood tests.

Experimental

Instrumentation

Preliminary collection of excitation and emission spectra was carried out with a commercial spectrofluorimeter (Photon Technology International). For steady state (SS) measurements, the excitation source was a continuous-wave 75-W xenon lamp with broadband illumination from 200 to 2000 nm. Detection was made with a photomultiplier tube (PMT; Model 1527) with wavelength range from 185 to 650 nm. The method of detection was analog for high signal levels or photon counting for low signal levels. In analog mode, the inherent peak to peak noise was 50×10^{-12} A with a 0.05-ms time constant. In photon counting mode, the maximum count rate was 4 MHz, pulse pair resolution was 250 ns, the rise time was 20 ns, and the fall time was 100 ns with a 220-ns pulse width. For time-resolved (TR) measurements, the excitation source was a pulsed 75-W xenon lamp (wavelength range from 200 to 2000 nm) with a variable repetition rate from 0 to 100 pulses per second and a pulse width of approximately 3 μs. Detection was by means of a gated analog PMT (Model R928) with extended wavelength range from 185 to 900 nm. SS and TR spectra were collected with excitation and emission monochromators having the same reciprocal linear dispersion (4 nm mm^{-1}) and accuracy (±1 nm with 0.25-nm resolution). Their 1200-grooves/mm gratings were blazed at 300 and 400 nm, respectively. The instrument was computer controlled using commercial software (Felix32) specifically designed for the system. Spectra were not corrected for instrumental response. Wavelength reproducibility was approximately ±2 nm.

Luminescence lifetimes were measured with an instrumental setup mounted in our laboratory [21]. Samples were excited by directing the output of a Northern Lights tunable dye laser (Dakota Technologies) through a KDP frequency-doubling crystal. The dye laser was operated on LDS 698 (Exiton) and pumped with the second harmonic of a 10-Hz Nd:YAG Q-switched solid-state laser (Big Sky Laser Technologies). Luminescence was detected with a multichannel detector consisting of a front-illuminated intensified-charge fiber-coupled device (ICCD; Andor Technology). The minimum gate time (full width at half maximum) of the intensifier was 2 ns. The CCD had the following specifications: active area = 690 × 256 pixels (26 mm^2 pixel size photocathode), dark current = 0.002 electrons/pixel/s, and readout noise = 4 electrons at 20 kHz. The ICCD was mounted at the exit focal plane of a spectrograph (SPEX 270M) equipped with a 1200-grooves/mm grating blazed at 500 nm. The system was used in the external trigger mode. The gating parameters (gate delay, gate width, and the gate step) were controlled with a digital delay generator (DG535; Stanford Research Systems) via a GPIB interface. Custom LabView software (National Instruments) was developed in-house for complete instrumental control and data collection. This system was also used to collect wavelength–time matrices for the analysis of target proteins in binary mixtures.

Reagents

All reagents and solvents were purchased from commercial suppliers and used without further purification. Nanopure water was used throughout. The organic solvents used in the synthesis were of HPLC grade. Anhydrous solvents were obtained by distillation of the HPLC-grade solvents over CaH_2.

Synthesis of the complexes

The syntheses of the complexes use the selectively hydrolyzed EDTA ester **1** [22]. The carboxylic acid

[2] *Abbreviations used:* CA, carbonic anhydrase; HSA, human serum albumin; PLS, partial least squares; SS, steady state; PMT, photomultiplier tube; TR, time-resolved; ICCD, intensified-charge fiber-coupled device; CCD, charge-coupled device; DCC, dicyclohexyl carbodiimide; NHS, *N*-hydroxysuccinimide; DMF, dimethylformamide; THF, tetrahydrofuran; As, aminosalicyclic acid; LOD, limit of detection; LDR, liner dynamic range; RSD, relative standard deviation.

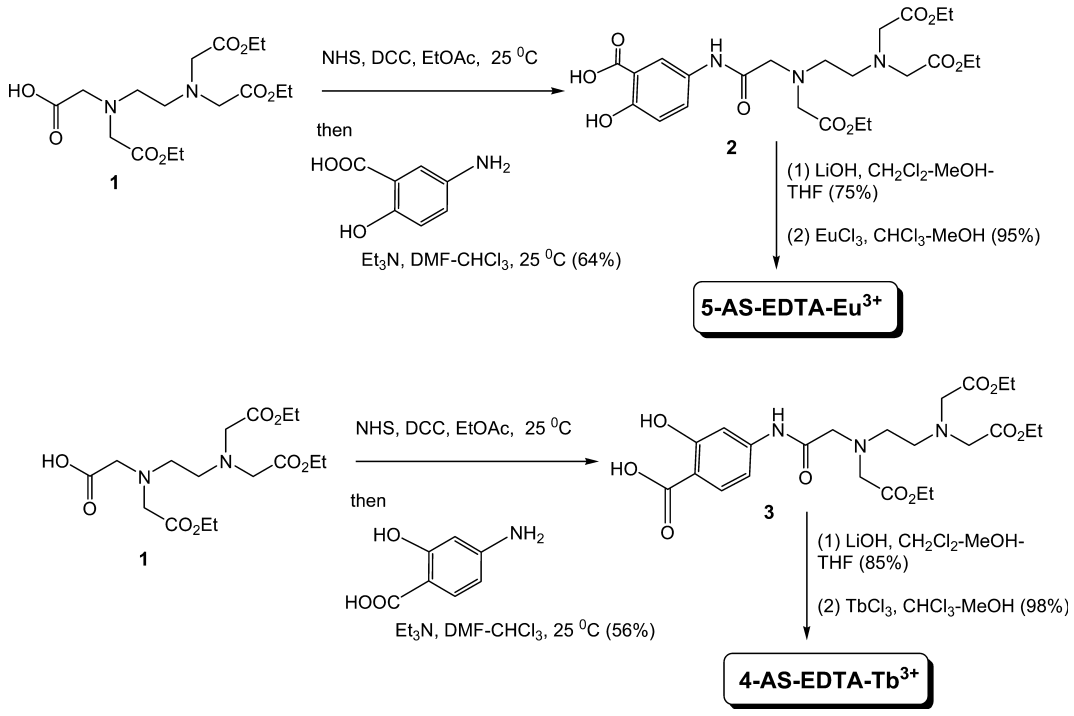

Scheme 1. Syntheses of the complexes 5As-EDTA-Eu^{3+} and 4As-EDTA-Tb^{3+}.

was activated with *N*-hydroxysuccinimide (NHS) and dicyclohexyl carbodiimide (DCC). The active ester was then reacted with the unprotected aminosalicylic (As) acids. We found this two-step procedure to give higher yields of the desired products (**2** and **3**) compared to the one-step coupling reactions. The ester groups were then hydrolyzed and the free acids were reacted with $EuCl_3$ or $TbCl_3$ to obtain the corresponding complexes. The synthetic steps are detailed in Scheme 1.

Compound 2

EDTA ester **1** [22] (1.10 g, 2.92 mmol) was dissolved in dry ethyl acetate (30 mL) and followed by the addition of NHS (0.37 g, 3.22 mmol) and DCC (0.665 g, 3.22 mmol) at room temperature. Stirring was continued at room temperature for another 12 h. The white precipitate was filtered under nitrogen and residue was washed with ice-cold ethyl acetate. Solvent was removed in vacuo. The viscous liquid was again dissolved in dry $CHCl_3$ (25 mL). 5-Amino salicylic acid-HCl-salt (0.470 g, 3.07 mmol) was dissolved in DMF (5 mL) in presence of Et_3N (0.7 mL, 5.03 mmol) and added dropwise. The reaction mixture was stirred at room temperature for 10 h and quenched with water. The organic layer was washed with water and dried over Na_2SO_4. The crude product was purified by silica gel column chromatography with 15% MeOH in $CHCl_3$ ($R_f = 0.2$). Yield: 0.67 g (82%, with respect to consumed **1**). ^1H NMR (500 MHz, $CDCl_3$) δ 1.39 (t, 9H, $J = 7.2$ Hz), 2.78–2.95 (m, 4H), 3.49 (s, 2H), 3.58 (s, 6H), 4.20 (q, 4H, $J = 7.2$ Hz), 4.25 (q, 2H, $J = 7.2$ Hz), 4.34–4.38 (bs, 1H), 6.89 (d, 1H, $J = 8.6$ Hz), 8.64 (dd, 1H, $J = 2.7$ and 8.6 Hz), 8.12 (d, 1H, $J = 2.7$ Hz).

5As-EDTA-Eu^{3+}

Compound **2** (0.14 g, 0.27 mmol) was dissolved in CH_2Cl_2/THF/MeOH (2/4/2 mL) and solid LiOH (85 mg, 2.02 mmol) was added. The reaction mixture was stirred at room temperature for 15 h. The pH of the solution was lowered by conc. HCl to 3.0. Solvent was removed in vacuo and the residue was again dissolved in minimum volume MeOH (300 μL) and THF/CH_2Cl_2 (2/2 mL) was added. The white precipitated was filtered off. Yield: 95 mg (69%). ^1H NMR (300 MHz, D_2O) δ 3.29–3.34 (m, 2H), 3.47–3.53 (m, 2H), 3.71 (s, 2H), 3.79 (s, 2H), 3.90 (s, 4H), 6.95 (d, 1H, $J = 8.8$ Hz), 7.51 (dd, 1H, $J = 3.0$ and 8.8 Hz), 7.86 (d, 1H, $J = 3.0$ Hz).

This acid (41 mg, 0.082 mmol) was dissolved in 5 mL of nanopure water and solid $EuCl_3 \cdot 6H_2O$ (30 mg, 0.082 mmol) was added. It was refluxed for 4 h and the solvent was removed in vacuo to afford changing it to produce a white powder. This powder was extensively washed with ether and cold methanol to obtain the complex (54 mg, 86%) as a white solid. Anal. Calcd. For $C_{17}H_{18}EuN_3O_{10} \cdot 3H_2O$: C, 32.39; H, 3.84; N, 6.67. Found: C, 32.55; H, 4.01; N, 6.52.

Compound 3

To a stirred solution of **1** (1.87 g, 4.97 mmol) in ethyl acetate (25 mL), DCC (1.2 g, 5.81 mmol), and NHS (0.63 g, 5.81 mmol) were added at 0 °C. Stirring was continued at this temperature for 1 h. The solid precipitate was filtered under nitrogen and solvent was removed from the clear filtrate under reduced pressure. The residue was dissolved in chloroform. To a suspension of 4-aminosalicylic acid (0.84 g, 5.47 mmol) in $CHCl_3$/DMF (30/5 mL), triethylamine (0.83 mL, 5.91 mmol) was added. The resulting solution was added to the chloroform solution of the residue and stirred at room temperature for 30 min and then at 50 °C for 12 h. The reaction mixture was then washed with brine and water and dried over Na_2SO_4, and the solvent was evaporated under reduced pressure. The crude product was purified by silica gel column chromatography (eluting with chloroform and then with 10% methanol in chloroform). Yield: 1.1 g (80%); $R_f = 0.2$ (15% MeOH in $CHCl_3$). ^{1}H NMR (500 MHz, $CDCl_3$) δ 1.24 (m, 9H), 2.86 (s, 4H), 3.52 (m, 8H), 4.14 (m, 6H), 7.23 (m, 1H), 7.40 (s, 1H), 7.81 (m,1H), 10.34 (s, 1H).

4As-EDTA-Tb^{3+}

The conjugate **3** (0.24 g, 0.47 mmol) was taken into THF-CH_2Cl_2-MeOH (4/4/8 mL) mixture. Solid LiOH (0.14 g, 5.83 mmol) was added to it and the reaction mixture was stirred at room temperature for 12 h. The solvent was evaporated under reduced pressure; the residue was dissolved in minimum quantity of absolute ethanol and precipitated by adding CH_2Cl_2. The precipitate was filtered, washed with CH_2Cl_2 and dried under vacuum yielding the tetraacid as a white solid (145 mg, 62%). ^{1}H NMR (500 MHz, D_2O) δ 3.36 (m, 2H), 3.54 (m, 2H), 3.95 (m, 8H), 7.09 (d, 1H, $J = 3.5$ Hz), 7.25 (s, 1H), 7.87 (d, 1H, $J = 3.5$ Hz).

The EDTA tetraacid (46 mg, 0.11 mmol) was dissolved in MeOH (2 mL). A solution of $TbCl_3 \cdot 6\ H_2O$ (40 mg, 0.11 mmol) in MeOH (1 mL) was added to it and the mixture was refluxed for 5 h. The solvent was removed in vacuo to afford changing it to produce a white powder. This powder was extensively washed with ether and cold methanol to obtain the complex (56 mg, 88%) as a white solid. Anal. Calcd. For $C_{17}H_{18}N_3O_{10}Tb \cdot 3H_2O$: C, 32.04; H, 3.80; N, 6.59. Found: C, 31.84; H, 3.75; N, 6.82.

Procedures

Measurements with the spectrofluorimeter were made with standard quartz cuvettes (1 × 1 cm). A fiber optic probe was used with the laser system. The probe assembly consisted of one excitation and six collection fibers fed into a 1.25-m section of copper tubing that provided mechanical support. All of the fibers were 3-m-long and 500-μm-core-diameter silica-clad silica with polyimide buffer coating (Polymicro Technologies). At the analysis end, the excitation and emission fibers were arranged in a conventional six-around-one configuration, bundled with vacuum epoxy (Torr-Seal, Varian) and fed into a metal sleeve for mechanical support. The copper tubing was flared, stopping at a swage nut tapped to allow for the threading of a 0.75-ml polypropylene sample vial. At the instrument end, the excitation fiber was positioned in an ST connection and aligned with the beam of the tunable dye laser while the emission fibers were bundled with vacuum epoxy in a slit configuration, fed into a metal sleeve, and aligned with the entrance slit of the spectrometer.

Luminescence lifetimes were determined via a three-step procedure [21]: (1) collection of full sample and background wavelength–time matrices, (2) subtraction of background decay curve from the luminescence decay curve at the target wavelengths of the sensor, and (3) fitting of the background-corrected data to single exponential decays. The decay curve data were collected with a minimum 300-μs interval between the opening of the ICCD gate and the rising edge of the laser pulse, which was sufficient to avoid the need to consider convolution of the laser pulse with the analyte signal (laser pulse width = 5 ns). In addition, the 300-μs delay completely removed the fluorescence of the sample matrix from the measurement. Fitted decay curves ($y = y_0 + A_1 \exp^{-(x-x_0)/t_1}$) were obtained with Origin software (version 5; Microcal Software) by fixing y_0 and x_0 at a value of zero. For chemometric analysis, all spectra were saved in ASCII format and transferred to a PC AMD 1200 MHz for subsequent manipulation. All chemometric calculations were done using MATLAB 6.0 [23]. PLS-1 was implemented using the MVC1 MATLAB toolbox [24].

Results and discussion

The luminescence of lanthanide ions, particularly Eu^{3+} and Tb^{3+}, has been extensively investigated [25–27]. Their long-lived luminescence provides ample opportunity to discriminate against short-lived background fluorescence and scattered excitation light. This is particularly attractive for bioassays because time-resolved measurements avoid strong fluorescence interference from biological matrices. Offsetting this advantage is the fact that lanthanide's luminescence is quite weak as a result of low molar extinction coefficients in aqueous solvents. Water molecules strongly bind to the lanthanide ion and quench its luminescence via weak vibronic coupling with the vibrational states of the O-H oscillators.

Significant enhancements for analytical use can be obtained with chelating agents that remove water molecules from the lanthanide's primary coordination sphere. Coordination of a chelating agent to the lantha-

nide ion also provides the possibility to attach a sensitizer (or antenna) to further enhance the luminescence of the lanthanide ion. Sensitizers are typically organic molecules that strongly absorb and transfer excitation energy to the metal ion, thereby overcoming the inherently weak absorption of the lanthanide ion.

For the purpose of this work, we chose ethylenediaminetetraacetic acid (EDTA) as the chelating agent. EDTA forms tightly bound complexes with Eu^{3+} and Tb^{3+} (binding constants being reported as ca. 10^{15} at pH 7) [28], which assure the physical integrity of the probes in the presence of potentially competing ions and/or proteins. 4-Aminosalicylic acid (4As) and 5-aminosalicylic acid (5As) were chosen as the antennas for Tb^{3+} and Eu^{3+} because their fluorescence spectra overlap the excitation spectra of the respective EDTA complexes. This is a recommended selection criterion for intramolecular energy transfer between an organic sensitizer and a lanthanide ion [25–27].

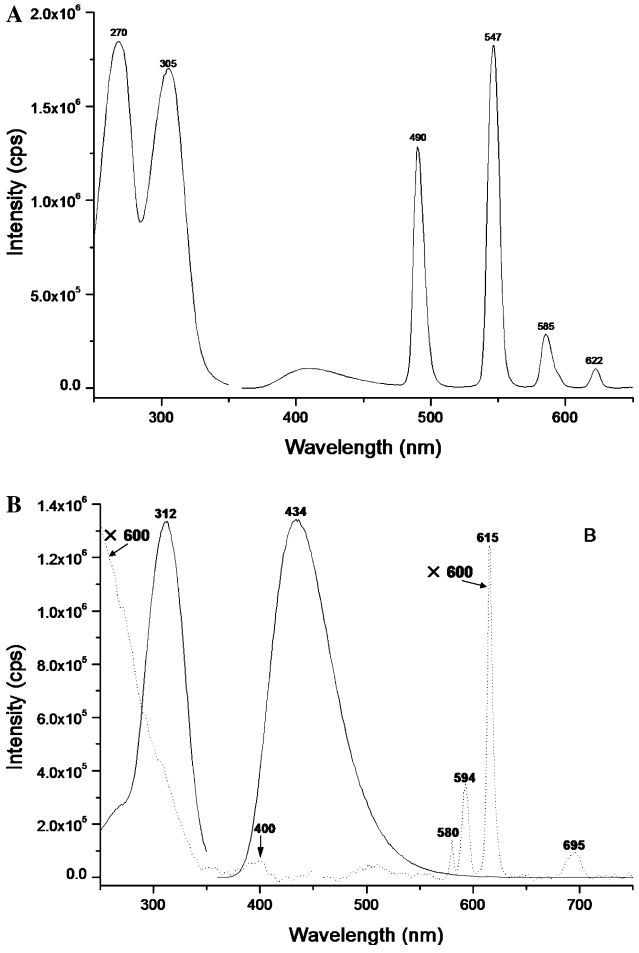

Fig. 1. Excitation and luminescence spectra of (A) 1.0×10^{-5} M 4As-EDTA-Tb^{3+} and (B) 1.0×10^{-5} M 5As-EDTA-Eu^{3+} in 25 mM Hepes recorded under (——) SS and (- - -) TR conditions. Instrumental parameters were as follows: (——) 2 nm excitation and emission band-pass; (- - -) delay time = 300 μs, gate time = 1000 μs, excitation (15 nm) and emission (2 nm) band-pass.

Fig. 1A shows the steady state excitation and luminescence spectra of 4As-EDTA-Tb^{3+}. The four sharp peaks that appear in the luminescence spectrum of the complex correspond to characteristic electronic transitions of the lanthanide ion [25–27]. Upon sample excitation at 270 nm, the luminescence intensity of 4As-EDTA-Tb^{3+} is approximately 1.4×10^2 higher than that from EDTA-Tb^{3+} (data not shown). This is attributed to energy transfer from 4As to Tb^{3+}. Fig. 1B shows the SS and the time-resolved excitation and luminescence spectra of 5As-EDTA-Eu^{3+}. In this case, the luminescence enhancement promoted by energy transfer is much lower than that observed in the Tb^{3+} complex. The broad emission band in the SS spectrum of 5As-EDTA-Eu^{3+} corresponds to the fluorescence contribution of the antenna. The luminescence of Eu^{3+} appears only in the TR spectrum of the complex. A 300-μs delay after the excitation pulse removes the fluorescence contribution from 5As and provides a reference signal solely based on the luminescence of Eu^{3+}.

Number of available sites for protein interaction in the first coordination sphere of the lanthanide ion

Luminescence quenching of lanthanide ions in aqueous solvents takes place via weak vibronic coupling with the vibrational states of the O-H oscillators [25,26]. Because O-H groups act independently, the overall effect on the rate of radiationless deactivation of the excited state is proportional to the number of O-H oscillators coordinated to the inner coordination sphere of the lanthanide ion. The replacement of O-H oscillators by lower-frequency oscillators, such as O–D oscillators, makes the vibronic deactivation pathway much less efficient. As a consequence, the luminescence lifetime of the excited state becomes considerably longer. This effect can be used to determine the number of water molecules coordinated to the lanthanide ion. According to Horrocks and Sundnick [27], the number of water molecules (q) is given by the equation $q = A_{LN}(\tau_{H_2O}^{-1} - \tau_{D_2O}^{-1})$, where A_{LN} is the proportionality constant for the lanthanide ion and τ_{H_2O} and τ_{D_2O} are the luminescence lifetimes of the lanthanide ion in H_2O and D_2O, respectively. A_{LN} values for Tb^{3+} and Eu^{3+} have been reported as 1.05 and 4.2, respectively [27].

Our lifetime experiments were carried out with complex solutions prepared in aqueous buffer (25 mM Hepes) or in aqueous buffer–D_2O mixtures containing different volume ratios of H_2O–D_2O. Measurements were made at the maximum excitation and emission wavelengths ($\lambda_{exc}/\lambda_{em}$) of the complexes; i.e., $\lambda_{exc}/\lambda_{em} = 305/547$ nm for 4As-EDTA-Tb^{3+} and $\lambda_{exc}/\lambda_{em} = 312/615$ nm for 5As-EDTA-Eu^{3+}. The lifetime in water was obtained from the average of six independent measurements directly taken from the complex in aqueous buffer (25 mM Hepes). τ_{D_2O} was obtained

experimentally and from extrapolation of the linear plot between the experimental reciprocal luminescence lifetime (τ^{-1}) and the mole fraction of water (χ_{H_2O}) in H_2O–D_2O mixtures (see Fig. 2A). The agreement between the experimental ($\tau^{-1} = 0.559\ ms^{-1}$) and the extrapolated ($\tau^{-1} = 0.565\ ms^{-1}$) values was excellent. The numbers of coordinated water molecules were calculated as 3.06 (5As-EDTA-Eu^{3+}) and 2.95 (4As-EDTA-Tb^{3+}). Therefore, the maximum number of available sites for protein–metal interaction can be approximated to three in both complexes. These numbers are in good agreement with the fact that EDTA was synthesized to coordinate five sites of the lanthanide ion and that Eu^{3+} and Tb^{3+} can take up to eight or nine molecules in their first coordination sphere. Fig. 2B shows the effect of D_2O on the luminescence intensity

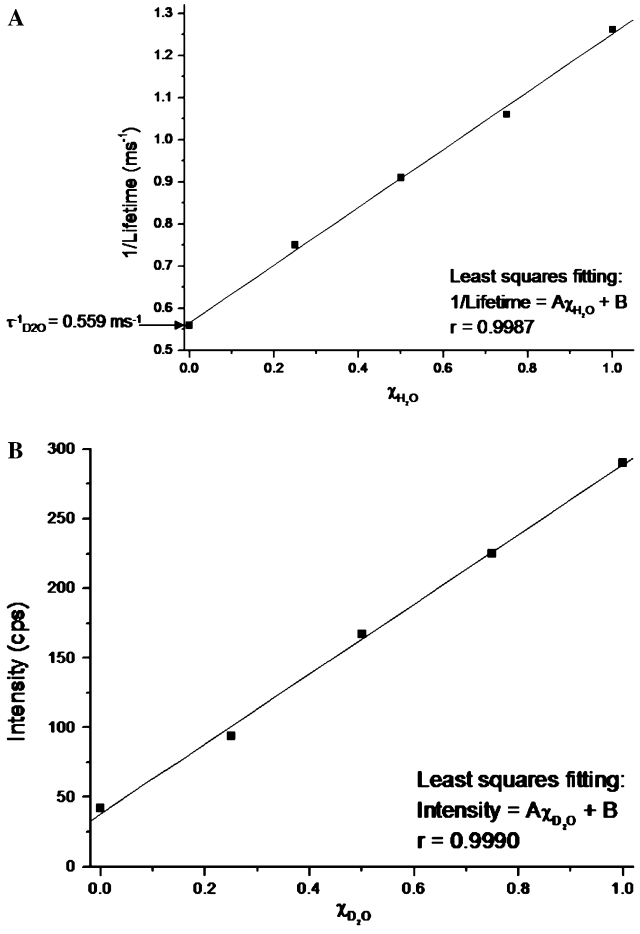

Fig. 2. (A) Reciprocal luminescence lifetime (τ^{-1}) in ms^{-1} as a function of mole fraction of water (χ_{H_2O}) in D_2O–H_2O mixtures in 2×10^{-9} M 4As-EDTA-Tb^{3+} solution (25 mM Hepes). $A = 0.6864\ ms^{-1}$ and $B = \tau^{-1}_{D_2O} = 0.565\ ms^{-1}$. Lifetime measurements were performed at $\lambda_{exc}/\lambda_{em} = 310/545$ nm. (B) Luminescence intensity of 5.0×10^{-6} M 5As-EDTA-Eu^{3+} (25 mM Hepes) as a function of mole fraction of D_2O. Intensity measurements were done at $\lambda_{exc}/\lambda_{em} = 316/615$ nm. $A = 250.8\ cps^{-1}$and $B = 38.2$ cps. All measurements were done using a 300- and 1000-μs delay and gate times, respectively.

of 5As-EDTA-Eu^{3+}. The maximum intensities were observed in the absence of water ($\chi_{D_2O} = 1$). The same type of behavior was observed with 4As-EDTA-Tb^{3+}. Assuming that O-H oscillators are replaced by lower-frequency oscillators in metal–protein interactions, the presence of the protein should enhance the luminescence intensity of the lanthanide complex.

Quantitative potential for protein analysis

The limit of detection (LOD) of an analytical method is directly related to the smallest measure that can be detected with reasonable certainty. The smallest discernable signal (x_L) is typically calculated by $x_L = x_B + ks_B$, where x_B is the main average of blank responses, s_B is the standard deviation of blank measurements, and k is a numerical factor chosen in accordance to the desired confidence level [28]. Therefore, to obtain the best LOD with a specific analytical method, it is convenient to reduce the blank signal to the minimum possible value. Because our approach is based on luminescence changes upon protein interaction with the lanthanide ion, our LOD also depends on the magnitude (x_R) and reproducibility (s_R) of the reference signal, i.e., the luminescence of the lanthanide ion in the absence of protein.

With the aid of an appropriate delay (300 μs) after the excitation pulse, our approach eliminates fluorescence background from biological matrices. Blank measurements detect only instrumental noise and the reference signal is free from fluorescence matrix interference. Instrumental noise becomes a problem only if the magnitude of the reference signal is close to that of instrumental noise. Because the concentration of the lanthanide complex is directly proportional to the reference signal, one can optimize the reproducibility of measurements and the LOD with the appropriate standard concentration. In doing so, one should also keep in mind that there is a direct correlation between standard and protein concentrations and protein traces are detected only with relatively low complex concentrations. Careful investigation of these parameters led us to set working concentrations at 2×10^{-9} M (4As-EDTA-Tb^{3+}) and 5×10^{-6} M (5As-EDTA-Eu^{3+}). The lower working concentration of 4As-EDTA-Tb^{3+} reflects the higher luminescence enhancement promoted by the energy transfer between 4As and Tb^{3+}. Although this complex is potentially more sensitive than 5As-EDTA-Eu^{3+}, its luminescence signal in the presence of proteins decays considerably upon irradiation time in the sample compartment of the spectrofluorimeter. For quantitative analysis, which is based on luminescence intensity, this behavior is not a problem because the analyst can always measure reproducible signals by setting a constant number of excitation pulses. On the other end, it becomes a problem when measuring luminescence decays

because it provides inaccurate lifetime values. Since our approach bases qualitative analysis on lifetime measurements, we decided to drop further investigations with 4As-EDTA-Tb^{3+}.

Fig. 3A shows the calibration curve of HSA obtained with 5×10^{-6} M 5As-EDTA-Eu^{3+}. The experiments were performed in batch (25 mM Hepes) and signal intensities were measured after 15 min of protein mixing. At this concentration, the signal-to-noise ratio of the reference signal was 3 and the relative standard deviation was 2.6% ($N = 16$). Clearly, there is a direct correlation between the luminescence intensity and the HSA concentration. Linear relationships were also obtained with CA and γ-globulin. Table 1 summarizes the analytical figures of merit obtained for these three proteins. The luminescence intensities plotted in the calibration graphs are the averages of individual measurements taken from three aliquots of the same working solution. The linear dynamic ranges (LDR) of the calibration curves are based on at least five protein concentrations. The lowest limit of the LDR corresponds to a concentration 3.3× the LOD. Because the presence of protein enhances the luminescence of Eu^{3+} and does not deteriorate the precision of measurements, the relative standard deviation (RSD) at the lowest limit of the LDR is better than 2.6%, i.e., the RSD of the reference value. The correlation coefficients and the slopes of the log–log plots (data not shown) are close to unity, demonstrating a linear relationship between protein concentration and signal intensity. The LOD were calculated with the equation $\mathrm{LOD} = 3s_R/m$; where m is the slope of the calibration curve and s_R is based on 16 measurements of the reference signal. A straightforward comparison with reported LOD for these three proteins is difficult because different instrumental setups and experimental and mathematical approaches have been used for their determination. However, we can safely state that our LOD are of the same order of magnitude as those previously reported with the most sensitive methods [11–17].

Table 1
Analytical figures of merit[a] for three proteins obtained with 5As-EDTA-Eu^{3+}

Protein	LDR (μg mL^{-1})[b]	R[c]	LOD (ng mL^{-1})[d]
HSA	0.86–35.0	0.9992	26
CA	3.20–43.1	0.9996	97
γ-Globulin	1.68–25.1	0.9998	56

[a] Measurements were made in 25 mM Hepes using excitation and emission wavelengths of 316 and 616 nm, respectively. Excitation and emission slits were 15 and 10 nm, respectively. Delay and gate times were 300 μs and 1 ms, respectively.
[b] LDR, linear dynamic range.
[c] R, correlation coefficient.
[d] LOD, limit of detection.

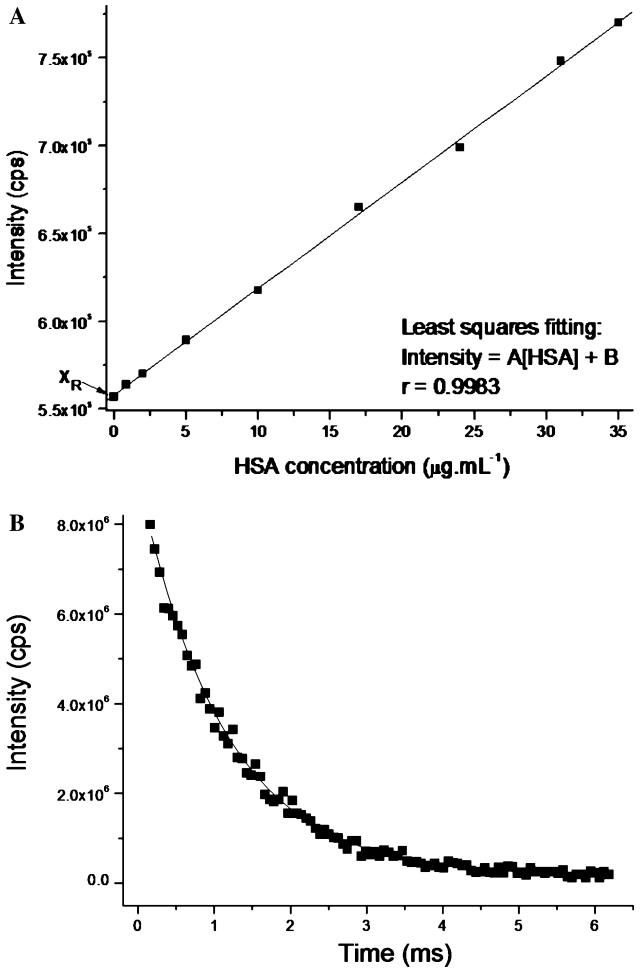

Fig. 3. (A) Calibration curve for HSA obtained with 5×10^{-6} M 5As-EDTA-Eu^{3+} in 25 mM Hepes. Intensity measurements were done at $\lambda_{exc}/\lambda_{em} = 316/615$ nm using 0.03- and 1000-ms delay and gate times, respectively. X_R = reference signal; $A = 6066$ mL μg^{-1} cps^{-1} and $B = 557{,}990$ cps^{-1}. (B) Fitted luminescence decay curve for 5×10^{-6} M 5As-EDTA-Eu^{3+} in the presence of 35 μg mL^{-1} HSA. Mixture was prepared in 25 mM Hepes. Experimental parameters for wavelength–time matrix collection were the following: $\lambda_{exc}/\lambda_{em} = 316/615$ nm; initial delay = 0.03 ms; gate width = 0.5 ms; gate step = 0.06 ms; number of accumulations per spectrum = 100 laser pulses; number of kinetic series per wavelength–time matrix = 40; slit width of spectrograph: 10 mm.

Qualitative potential of 5As-EDTA-Eu^{3+}

The replacement of O-H oscillators by the O-D variety causes a significant change in the luminescence lifetime of the complex. Assuming a similar effect upon protein binding, we investigated the possibility of using luminescence lifetime for protein identification. The experiments were carried out in batch (25 mM Hepes) with a 5×10^{-6} M final concentration of 5As-EDTA-Eu^{3+} in the analytical sample. The exponential decays were collected at $\lambda_{exc}/\lambda_{em} = 312/615$ nm after 15 min of protein mixing. Protein concentrations in the final mixtures varied within the LDR of the calibration curves.

Fig. 3B shows a typical decay in the presence of 35 μg mL^{-1} HSA, i.e., a protein concentration at the upper limit concentration of the LDR (see Table 1). The agreement between the calculated and the observed points over the two lifetimes of the decays agreed to within about 1% and the residuals showed no systematic trends. Single exponential decays with excellent fittings were also observed in the presence of 43.1 ng mL^{-1} CA and 25.1 ng mL^{-1} γ-globulin. The single exponential decays suggest that only one type of microenvironment per protein surrounds Eu^{3+} or that only one type of microenvironment significantly contributes to the measured lifetime. Table 2 compares the reference lifetime (absence of protein) to the lifetimes in the presence of the three proteins. For a confidence level of 95% ($\alpha = 0.05$; $N_1 = N_2 = 6$) [28], the reference value was statistically different from the lifetime in the presence of the three proteins, demonstrating that the lifetime of the complex is sufficiently sensitive to detect the presence of these proteins. The lifetime in the presence of CA was significantly different ($p = 0.05$; $N_1 = N_2 = 6$) from the lifetimes in the presence of the other two proteins. The same is true for HSA and γ-globulin, which demonstrates the possibility of using the complex to identify any one of these proteins in the presence of the other two. The lifetimes in the presence of the three proteins are significantly longer than the lifetime in the absence of proteins. This is in agreement with the luminescence enhancement observed upon protein interaction with the complex and the assumption that their interactions substitute the O-H oscillators of water molecules with lower-frequency oscillators in the inner coordination sphere of Eu^{3+}. The difference in lifetime values may be ascribed to structural differences of the three proteins [17,18]. Although HSA and CA have both α helix and β sheet structure, CA has mostly β sheet structure. γ-Globulin has only β sheet structure. HSA and CA are hydrophilic types of proteins and γ-globulin is a hydrophobic type of protein [17,18].

Table 2
Comparison of luminescence lifetimes measured with 5As-EDTA-Eu^{3+} in the absence and the presence of proteins

Protein[a]	Lifetime[b] (μs)	RSD[c] (%)
—	210 ± 5	2.4
HSA	288 ± 6	2.1
CA	259 ± 5	1.9
γ-Globulin	232 ± 6	2.8

[a] Protein solutions were mixed with 5×10^{-6} M complex to provide the following final concentrations: 35 μg mL^{-1} HSA, 43.1 ng mL^{-1} CA, and 25.1 ng mL^{-1} γ-globulin. All solutions were prepared in 25 mM Hepes.

[b] Lifetimes are the average values of six measurements taken from six aliquots of sample solution. All measurements were made at $\lambda_{exc}/\lambda_{em} = 316/615$ nm.

[c] RSD, relative standard deviations of luminescence lifetimes.

Simultaneous determination of HSA and γ-globulin in binary mixtures

Our approach bases quantitative analysis on the linear relationship between signal intensity and protein concentration. Because there is no spectral shift upon protein interaction, the qualitative parameter for protein identification is the luminescence lifetime. Unless the target protein is the only protein in the analytical sample, these two parameters should be simultaneously considered to achieve accurate qualitative and quantitative analysis. In this section, we demonstrate the feasibility of determining the concentration of HSA and γ-globulin in binary mixtures using a chemometric model to simultaneously process signal intensity and lifetime data.

A variety of linear regression methods for multicomponent analysis have been proposed, among which the most popular is partial least squares (PLS). De facto, PLS has become the standard for multivariate calibration because of the quality of the calibration models, the ease of implementation, and the availability of commercial software [29–34]. In addition, PLS uses full data points, which is critical for the spectroscopic resolution of complex mixtures of analytes. It allows for a rapid determination of components, usually with no need for prior separation. An additional advantage of PLS is that calibration can be performed by ignoring the concentrations of all other components except the analyte of interest. PLS regression has already been used to predict the concentration of HSA and γ-globulin in binary mixtures, but protein determination was based on the differences observed in second-derivative near-infrared spectra [17,18]. In our case, PLS uses the luminescence lifetimes as discriminatory parameters and regresses the luminescence decays onto the concentrations of the standards.

The calibration set for chemometric analysis was built with a nine-sample set. The component concentrations corresponded to a three-level full-factorial design with protein concentrations ranging from 10 to 30 μg mL^{-1} HSA and from 10.0 to 20.0 μg mL^{-1} γ-globulin. The validation set was also built with a nine-sample three-level full-factorial design, but the component concentrations were different from those used for the calibration set. The fact that the component concentrations spanned the concentrations ranges of the calibration set allowed us to draw conclusions on the predictive ability of the implemented models. The decays for all sets were recorded in random order with respect to protein concentrations at $\lambda_{exc}/\lambda_{em} = 312/615$ nm.

Table 3 shows the time windows (or regions) of the luminescence decays and the optimum number of factors used for calibration, the root-mean-square error of cross-validation (RMSECV), and the relative error of prediction (REP %). The optimum number of fac-

Table 3
Statistical parameters obtained by PLS 1

Parameters	HSA	γ-Globulin
Region (μs)	30–3000 (50 data points)	30–3000 (50 data points)
Factors[a]	2	2
RMSECV[b] (μg/mL)	1.94	1.47
REP (%)[c]	9.9	10.1

[a] Factors were selected following the Haaland criterion [29].

[b] $\mathrm{RMSECV} = \sqrt{\frac{\sum (x_{\mathrm{act}} - x_{\mathrm{pred}})^2}{I}}$

[c] $\mathrm{REP}(\%) = \mathrm{RMSECV} \times 100/\bar{x}_{\mathrm{act}}$, where x_{act} is the actual concentration in calibration samples, x_{pred} is the predicted concentration with the PLS model and $\bar{x}_{\mathrm{act}}$ is the average concentration in the calibration set.

tors—which allows one to model the system with the optimum data volume avoiding overfitting—was determined with the cross-validation procedure. This procedure removes one training sample at a time and uses the remaining samples to build the latent factors and regression [29]. Table 4 shows the experimental results obtained from several binary samples with the optimized calibration set. The agreement between the predicted and the actual protein concentrations is excellent for both proteins, demonstrating the potential of the method to simultaneously distinguish and quantify both proteins in the studied concentration range.

Conclusion

The two lanthanide complexes present the appropriate spectral characteristics for the purpose at hand, i.e., to serve as luminescence reporters for liposome–protein interaction. Strong absorption from biological matrices typically occurs below 300 nm. The broad excitation spectra of 4As-EDTA-Tb^{3+} and 5As-EDTA-Eu^{3+} provide ample opportunity for finding an appropriate excitation wavelength with reduced primary inner filter effects. Our experiments were performed upon sample excitation at their maximum excitation wavelengths, but longer excitation wavelengths can certainly promote efficient energy transfer and reproducible reference signals. Their long luminescence lifetimes allow one to use a 300-μs delay after the excitation pulse and still collect strong luminescence from the probe. This delay is long enough to reduce short-lived fluorescence biological background to instrumental noise. As a consequence, both reference signals solely rely on the well-characterized luminescence spectra of the lanthanide ions. Because their spectral profile does not change upon chemical perturbation, protein determination is based on reliable reference signals. In both complexes, EDTA takes five coordination sites in the first coordination sphere of the lanthanide ion, forming tightly bound complexes. This is important to retain the physical integrity of the probe upon protein interaction.

Protein interaction enhances the luminescence signals of Tb^{3+} and Eu^{3+}. The observed luminescence enhancements are attributed to the removal of water molecules from the three remaining coordination sites of the lanthanide ion. There is a linear correlation between the concentration of the complex and the minimum protein concentration detected with the probe. The higher luminescence intensity of 4As-EDTA-Tb^{3+} provides a minimum working concentration—i.e., a complex concentration that still produces a reproducible reference signal—approximately three orders of magnitude lower than the working concentration of 5As-EDTA-Eu^{3+}. This fact makes 4As-EDTA-Tb^{3+} the more sensitive probe. Unfortunately, its luminescence intensity decays considerably upon sample excitation and makes it unsuitable for accurate lifetime analysis.

On the other end, 5As-EDTA-Eu^{3+} turned out to be a valuable probe for liposome–protein interaction. Based on its luminescence intensity, it was possible to

Table 4
Comparison of predicted and actual protein concentrations in binary mixtures

Validation samples	HSA			γ-Globulin		
	Actual	Predicted	Recovery (%)	Actual	Predicted	Recovery (%)
1	15.0	14.4	96.0	12.5	11.1	88.8
2	15.0	16.3	108.7	12.5	11.7	93.6
3	15.0	15.3	102.0	12.5	13.9	111.2
4	20.0	18.5	92.5	15.0	14.5	96.7
5	20.0	21.2	106.0	15.0	15.3	102.0
6	20.0	20.6	103.0	15.0	15.8	105.5
7	25.0	21.5	86.0	17.5	16.4	93.7
8	25.0	27.6	110.4	17.5	15.0	85.7
9	25.0	26.6	106.4	17.5	18.0	102.9
Average recovery (%)			101.2			97.8
Standard deviation			8.1			8.3
RSD[a]			0.080			0.084

[a] RSD, relative standard deviation.

quantify CA, HSA, and γ-globulin at the parts per billion level. The concentration ranges examined in the present study cover the concentration values typically found for HSA, CA, and γ-globulin in clinical tests of human blood serum. Our LOD were of the same order of magnitude as those previously reported with the most sensitive methods [11–16,1]. Its luminescence decay, which followed well-behaved single exponential decays in the presence and the absence of proteins, provides a selective parameter for protein identification on the bases of lifetime analysis.

The combination of luminescence intensities and decays with a PLS calibration model made feasible the direct determination of HSA and γ-globulin in binary mixtures. However, for the analysis of matrixes with higher complexity—such as those typically found in physiological fluids—an additional parameter for selectivity might be necessary to reduce potential interference from other proteins. Future studies in this direction will incorporate 5As-EDTA-Eu^{3+} into polymerized liposomes specifically designed to recognize a target protein in a complex matrix.

Acknowledgments

This research was supported by the National Institutes of General Medicine Science (NIH 1 RO1 GM 63204-01A1, to S.M. and A.C.) and the National Science Foundation (CHE-0138093 to A.C.).

References

[1] L.Y. Wang, Y.Y. Zhou, L. Wang, C.Q. Zhu, Y.X. Li, F. Gao, Synchronous fluorescence determination of protein with functionalized CdS nanoparticles as a fluorescence probe, Anal. Chim. Acta 466 (2002) 87–92.

[2] O.H. Lowry, N.J. Rosebrough, R.J. Randall, Protein measurement with the folin phenol reagent, J. Biol. Chem. 193 (1951) 265–275.

[3] M.M. Bradford, A rapid and sensitive method for the quantification of microgram quantities of protein utilizing the principle of protein-dye binding, Anal. Biochem. 72 (1976) 248–254.

[4] T. Zor, Z. Selinger, Linearization of the Bradford protein assay increases its sensitivity: theoretical and experimental studies, Anal. Biochem. 236 (1996) 302–308.

[5] S.C. Chou, A.C. Goldstein, Chromogenic groupings in the lowry protein determination, Biochem. J. 75 (1960) 109–115.

[6] I. Mori, K. Taguch, Y. Fujita, T. Matsuo, Sensitive spectrophotometric determination of human serum albumin (HSA) with (2-(5-bromo-2-pyridylazo)-5-(*N*-phenyl-*N*-sulfopropylamino)phenol)-cobalt (III) complex, Anal. Lett. 28 (1995) 225–237.

[7] Y.X. Li, D.H. Zhao, C.Q. Zhu, L. Wang, J.G. Xu, Determination of proteins at nanogram levels by their quenching effect on the chemiluminescence reaction between luminol and hydrogen peroxide with manganese-tetrasulfonatophthalocyanine as a new catalyst, Anal. Bioanal. Chem. 374 (2002) 395–398.

[8] Z.P. Li, K.A. Li, S.Y. Tong, Study of the catalytic effect of copper (II)-protein complexes on luminal-H_2O_2 chemiluminescence reaction and its analytical application, Anal. Lett. 32 (1999) 901–913.

[9] C.Q. Ma, K.A. Li, S.Y. Tong, Determination of proteins by fluorescence quenching of Erithrosin B, Anal. Chim. Acta 333 (1996) 83–88.

[10] N. Li, K.A. Li, S.Y. Tong, Fluorimetric determination for micro amounts of albumin and globulin fractions without separation by alpha, beta, gamma, delta-tetra (4′-carboxyphenyl)porphin, Anal. Biochem. 233 (1996) 151–155.

[11] C.X. Yang, Y.F. Li, C.Z. Huang, Determination of proteins with fast red VP by a corrected resonance light scattering of toluidine blue, Anal. Sci. 19 (2003) 1483–1486.

[12] L.J. Dong, R.P. Jia, Q.F. Li, Quantitative determination of proteins by Rayleigh light scattering technique after optimization of the derivatization reaction with Arsenazo-DBS, Anal. Chim. Acta 459 (2002) 313–322.

[13] D.E. Terry, E. Umstot, D.M. Desiderio, Optimized sample-processing time and peptide recovery for the mass spectrometric analysis of protein digests, J. Am. Soc. Mass Spectr. 15 (2004) 784–794.

[14] A.M. Timperio, C.G. Huber, L. Zolla, Separation and identification of the light harvesting proteins contained in grana and stroma thylakoid membrane fractions, J. Chromatogr. A 10238 (2004) 77–84.

[15] T.W.M. Fan, R.M. Higashi, An electrophoretic profiling method for thiol-rich phytochelatins and metallothioneins, Phytochem. Anal. 15 (2004) 175–183.

[16] G.H. Zhou, G.A. Luo, G.A. Sun, Y.C. Cao, X.D. Zhang, X. Zhang, Characterization of recombinant human granulocyte colony stimulating factor (rHuG-CSF) by capillary zone electrophoresis, capillary isoelectric focusing electrophoresis and electrospray ionization mass spectrometry, J. Pharmaceut. Biomed. 35 (2004) 425–432.

[17] K. Murayama, K. Yamada, R. Tsenkova, Y. Wang, Y. Ozaki, Near-infrared spectra of serum albumin and γ-globulin and determination of their concentrations in phosphate buffer solutions by partial least squares regression, Vib. Spectrosc. 18 (1998) 33–40.

[18] S. Kasemsumran, Y.P. Du, K. Murayama, M. Huehne, Y. Ozaki, Near-infrared spectroscopic determination of human serum albumin, γ-globulin, and glucose in a control serum solution with searching combination moving window partial least squares, Anal. Chim. Acta 512 (2004) 223–230.

[19] B.C. Roy, Md. Abdul Fazal, A. Arruda, S. Mallik, A.D. Campiglia, Polymerized fluorescent liposomes incorporating lanthanide ions, Org. Lett. 2 (2000) 3067–3070.

[20] B.C. Roy, M. Santos, S. Mallik, A.D. Campiglia, Synthesis of metal-chelating lipids to sensitize lanthanide ions, J. Org. Chem. 68 (2003) 3999–4007.

[21] A.J. Bystol, A.D. Campiglia, G.D. Gillispie, Laser-induced multidimensional fluorescence spectroscopy in Shpol'skii matrixes with a fiber optic probe at liquid helium temperature, Anal. Chem. 73 (2001) 5762–5770.

[22] E. Burks, N. Koshti, H. Jacobs, A. Gopalan, Selective monohydrolysis of esters of polyaminocarboxylic acids using pig liver esterase, Synlett (1998) 1285–1287.

[23] MATLAB 6.0, The Math Works Inc., Natick, MA, 2000.

[24] A.C. Olivieri, H.C. Goicoechea, F. Iñón, MVC1: an integrated MATLAB toolbox for first-order multivariate calibration, Chemom. Intell. Lab. Syst. 73 (2004) 189–197.

[25] J. Siepak, Terbium chelate labels for fluorescence immunoassays, Analyst 114 (1989) 529–531.

[26] J. Georges, Lanthanide-sensitized luminescence and applications to the determination of organic analytes, Analyst 118 (1993) 1481–1486.

[27] W. De, W. Horrocks Jr., D.R. Sudnick, Lanthanide ion luminescence probes of the structure of biological macromolecules, Acc. Chem. Res. 14 (1981) 384–392.

[28] J.C. Miller, J.N. Miller, Statistics for Analytical Chemistry, Wiley, New York, 1984.

[29] E.V. Thomas, D.M. Haaland, Partial least-squares methods for spectral analyses. 1. Relation to other quantitative calibration methods and the extraction of qualitative information, Anal. Chem. 60 (1988) 1193–1202.
[30] H. Martens, T. Naes, Multivariate Calibration, Wiley, Chichester, 1989.
[31] M. Blanco, J. Coello, H. Iturriaga, S. Maspoch, C. De, la Pezuela, Quantitation of the active compound and major excipients in a pharmaceutical formulation by near infrared diffuse reflectance spectroscopy fibre optical probe, Anal. Chim. Acta 333 (1996) 147–156.
[32] J. Coello, S. Maspoch, N. Villegas, Simultaneous kinetic-spectrophotometric determination of levodopa and benserazide by bi- and three-way partial least squares calibration, Talanta 53 (2000) 627–637.
[33] T. Galeano Diaz, I. Durán Merás, A. Guiberteau Cabanillas, M.F. Alexandre Franco, Voltammetric behavior and determination of tocopherols with partial least squares calibration: analysis in vegetable oil samples, Anal. Chim. Acta 511 (2004) 231–238.
[34] A. Muñoz de la Peña, A. Espinosa Mansilla, M. Acedo Valenzuela, A.C. Olivieri, H.C. Goicoechea, Comparative study of net analyte signal-based methods and partial least squares for the simultaneous determination of amoxycillin and clavulanic acid by stopped-flow kinetic analysis, Anal. Chim. Acta 463 (2002) 75–88.